Mater.Phys.Mech.4 (2001) 34-38

THE EFFECT OF BORON CONTENT ON THE CRYSTALLIZATION BEHAVIOUR AND MICROSTRUCTURE FOR NANOCRYSTALLINE $Fe_{93-x}Zr_7B_x$ ALLOYS

X.Y. Xiong[1], T.R. Finlayson[2] and B.C. Muddle[2]

[1] Materials Engineering Laboratory, National Institute for Materials Science, 1-2-1 Sengen, Tsukuba 305-0047, Japan

[2] School of Physics and Materials Engineering, Monash University, P.O. Box 27, Clayton, Victoria, Australia, 3168

Received: June 11, 2001

Abstract. The crystallization behaviour of amorphous $Fe_{93-x}Zr_7B_x$ (x = 3, 6, 12 at.%) alloys and the microstructures of the primary crystallization products have been studied using a combination of differential scanning calorimetry, differential thermal analysis, x-ray diffraction and transmission electron microscopy. For x = 3 and 6 at.% the sole product of primary crystallization is the bcc α-Fe phase. The average grain size of the crystalline phase was 14 nm for the $Fe_{90}Zr_7B_3$ alloy heated to 875K at 20 K/min and 12 nm for the $Fe_{87}Zr_7B_6$ alloy heated to 893K at 20 K/min. However, when x = 12, primary crystallization results in a metastable phase with the cubic "$Fe_{12}Si_2ZrB$" structure and the α-Fe phase. The average grain size of this metastable phase was 35 nm for the alloy heated to 883K at 20 K/min. Transformation of this metastable phase to predominantly bcc α-Fe can be induced by isothermal heat treatment at sufficiently high temperatures.

1. INTRODUCTION

Nanocrystalline Fe-Zr-B alloys are of interest due to their high saturation magnetization and high magnetic permeability. Studies of the effects of boron on the formation of nanocrystalline structures and magnetic properties [1,2] have shown that the addition of boron to Fe-Zr alloys improves the glass-forming ability and refines the primary bcc α-Fe grains during crystallization, with an increased permeability. At 8 at.% boron, the magnetic permeability is decreased [2,3].

In this paper, we report studies of the crystallization behaviour of amorphous $Fe_{93-x}Zr_7B_x$ (x = 3, 6, 12 at.%) alloys.

2. EXPERIMENTAL METHODS

Amorphous $Fe_{93-x}Zr_7B_x$ (x = 3, 6, 12 at. %) alloy ribbons, 20 μm thick and 1 to 2 mm wide, were produced by melt-spinning (in a helium atmosphere) ingots prepared initially by argon-arc melting. The amorphous nature of the ribbons was confirmed by x-ray diffraction (XRD) and transmission electron microscopy (TEM). Differential thermal analysis (DTA) and differential scanning calorimetry (DSC) were used to investigate the crystallization of the ribbons. The microstructures of the crystallized alloys were examined using XRD and TEM. Samples for the latter were prepared by electropolishing in an electrolyte of 5% perchloric acid and 95% methanol at about -40 °C and at 14-18 V.

3. RESULTS AND DISCUSSION

DTA, DSC and XRD. Fig. 1 shows DTA curves measured at a heating rate 10 K/min. For each alloy there are two exothermic peaks, corresponding to two individual crystallization reactions, in agreement with the result reported for low boron content [B] alloys [1]. With increasing [B], the onset temperature of the first peak, T_{x1} (see Fig. 1), increased from 786K (at x = 3) to 822K (at x = 12) suggesting an improvement in the thermal stability of the amorphous phase with increasing [B]. However, the second peak temperature, T_{p2}, did not change significantly.

Corresponding author: Trevor R. Finlayson, e-mail: trevor.finlayson@spme.monash.edu.au

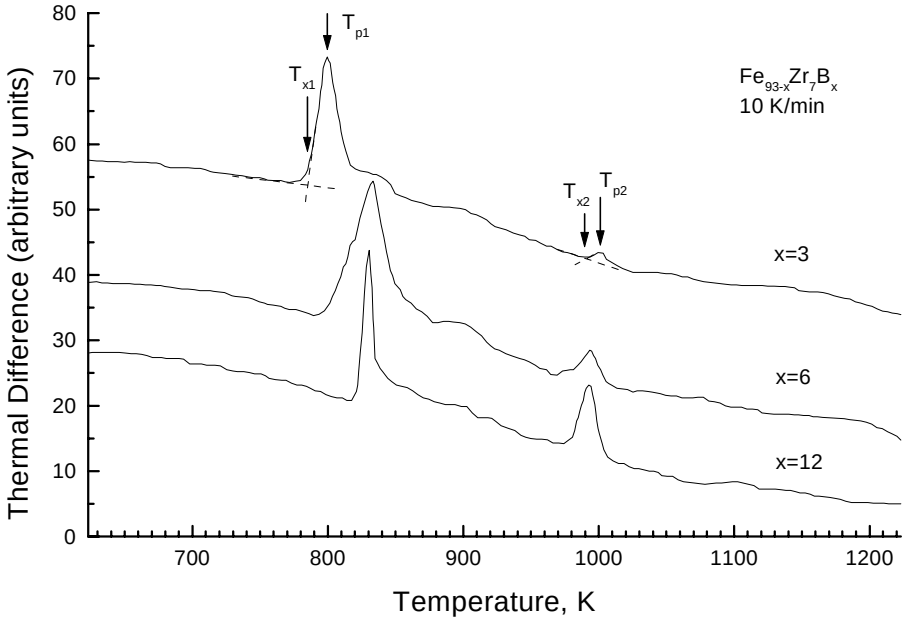

Fig. 1. Differential thermal analysis data for amorphous $Fe_{93-x}Zr_7B_x$ alloys.

The microstructure following primary crystallization is most significant for good soft magnetic properties [4]. Changes in microstructure were examined for the DSC samples, following rapid cooling from temperatures immediately before and after the crystallization peak and at the peak itself.

Fig. 2 shows the XRD results for the $Fe_{90}Zr_7B_3$ sample in the as-quenched state and after being heated to 753K (before the primary crystallization peak), 825K (at the primary crystallization peak), 875K (after the primary crystallization peak) and 1003K (after the second peak) at 20 K/min in the DSC sample holder. For the as-quenched sample, there was only one broad peak, with a 2θ width of about 10 degrees. For the sample heated to 753K, a small, sharp peak at 2θ = 44.6° indicating partial

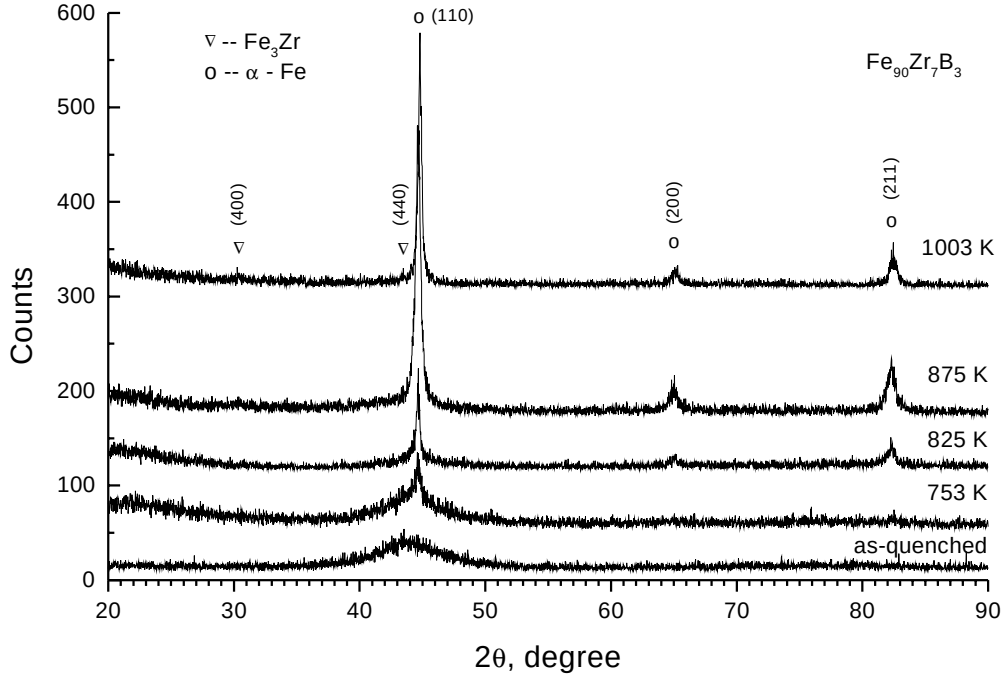

Fig. 2. XRD patterns for the $Fe_{90}Zr_7B_3$ samples in the as-quenched state and after being heated to temperatures as indicated, at 20 K/min.

crystallization, is evident. For the samples heated to 825K and 875K, there were three diffraction peaks, evidence of the bcc α-Fe phase. With increasing temperature, the intensities of the three α-Fe peaks increased, corresponding to the increase in the volume fraction of this phase. Upon increasing the temperature to 1003K, the (110) α-Fe peak became slightly narrower, suggesting that the grain size of the crystalline phase had increased, and two minor peaks emerged at $2\theta = 30.3°$ and 43.7°. These two peaks can be indexed as the fcc Fe_3Zr phase.

Using the Scherrer equation [5] and the full-widths-at-half-maximum for the (110) peaks following the 875K and 1003K heat treatments, the grain sizes of the bcc α-Fe phase were estimated to be 18 nm and 33 nm, respectively.

A similar pattern of crystallization behaviour, based on XRD observations, was found for the $x = 6$ alloy so that for both $Fe_{90}Zr_7B_3$ and $Fe_{87}Zr_7B_6$ amorphous alloys, the crystallization reaction is:

- amorphous → α-Fe + residual amorphous, for the primary crystallization;
- residual amorphous → α-Fe + Fe_3Zr, for the secondary crystallization;

in good agreement with previous reports for low [B] alloys [3,6].

However, at $x = 12$ the crystallization reaction was distinctively different, although this difference was not readily evident from the DTA or DSC curves. The general form of these curves was similar to those for the alloys of lower [B]s, but with the exotherm representing primary crystallization being sharper in profile (Fig. 1). Primary crystallization was clearly evident for a sample heated in the DSC to the primary crystallization peak temperature and quenched. The diffraction pattern for this sample could be indexed from the Powder Diffraction File (PDF) to a cubic phase with the "$Fe_{12}Si_2ZrB$" structure. For the samples heated to the higher temperatures and quenched (i.e., temperatures above that of the primary crystallization peak and below and above that for the secondary peak (Fig. 1)) the additional crystalline phases, bcc α-Fe and fcc $ZrFe_2$ also appeared.

This crystallization sequence was further studied by isothermal heat treatments on samples rapidly heated to temperatures just above the primary crystallization peak temperature. Samples were heated for 0.5, 2.0, 10, 24 and 240 h at 873K and 24 and 240 h at 973K. XRD on these samples showed that, given sufficient time, the primary crystallization product which was the cubic, "$Fe_{12}Si_2ZrB$" structure phase, transformed to predominantly bcc α-Fe and minority crystalline phases, fcc $ZrFe_2$, hcp Fe_2Zr and hcp ZrB_2.

In summary, the phase transformation sequence occurring at 973K in the $x = 12$ material can be summarized as follows:

- amorphous phase → "$Fe_{12}Si_2ZrB$" + residual amorphous phase, for primary crystallization;
- "$Fe_{12}Si_2ZrB$" + residual amorphous phase → α-Fe + Fe_2Zr + residual amorphous phase;
- Fe_2Zr + residual amorphous phase → α-Fe + ZrB_2.

These results are quite different from those reported by Kopcewicz *et al*. [7], who studied the microstructure and magnetic properties of the amorphous and nanocrystalline $Fe_{81}Zr_7B_{12}$ alloy and claimed that when the alloy was heated to 823K and 873K, the bcc α-Fe phase was formed, accompanied by $Fe_3(Zr,B)$ phase. However, in the present study, the XRD patterns for the samples heated to 849K and 883K cannot be indexed for either the α-Fe or $Fe_3(Zr,B)$ phases.

According to the equilibrium phase diagram of the Fe-Zr-B alloy system [8,9], the bcc α-Fe and fcc $ZrFe_2$ are equilibrium phases. However, there is no indication of a phase with the "$Fe_{12}Si_2ZrB$" structure. This phase must be metastable, even though it has been observed to be stable at 1003K used in the initial heat treatment studies conducted in the DSC facility. Each of the isothermal heat treatments has shown it to transform after sufficient time at temperature, above its initial temperature of formation. To the best of our knowledge, this is the first report of a metastable phase with the "$Fe_{12}Si_2ZrB$" structure to be observed in Fe-Zr-B alloys.

TEM Observations. TEM observations were carried out on selected XRD samples.

For the as-quenched sample of the $Fe_{90}Zr_7B_3$ alloy, a homogeneous structure was observed in the bright field (BF) image. The intensity distribution was quite even and no sharp contrast was observed in the field of view. A selected area diffraction (SAD) pattern only had a few concentric diffuse rings. Using a portion of the first strong diffuse ring to form a centered dark field (CDF) image, only speckled contrast was observed. No indication of the presence of crystalline structure was evident. These observations are consistent with results in the literature [6].

However, for a specimen heated to a temperature above that of the primary crystallization peak measured in the DSC, there was a dense distribution of crystalline grains, dispersed quite uniformly throughout an amorphous matrix. Following the complete primary crystallization reaction, as shown in Fig. 3, the grain size of the crystalline phase was typically in the range 10–30 nm. By counting about

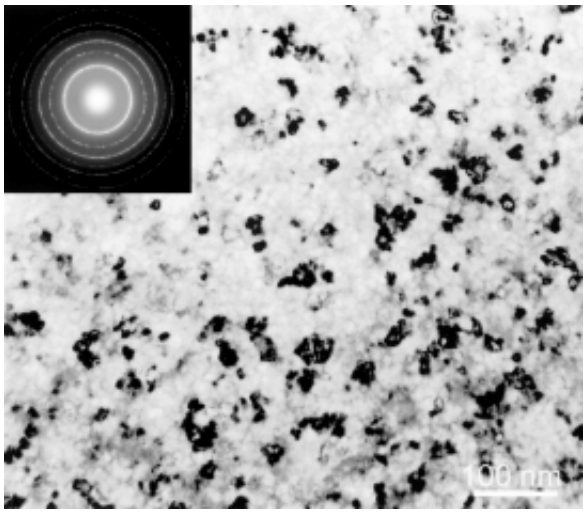

Fig. 3. TEM bright field image and corresponding SAD pattern for the nanocrystalline $Fe_{90}Zr_7B_3$ alloy heated to 875K at 20 K/min.

150 grains and using the normal distribution curve to fit the grain size data, the average grain size was determined to be 14 nm for the sample heated to 875K, which is in fairly good agreement with the x-ray line width value of 18 nm.

Analysis of the SAD pattern (Fig. 3) confirmed that the crystalline phase was bcc α-Fe, which is consistent with the XRD result shown in Fig. 2.

Similar results were found from TEM on samples of the $Fe_{87}Zr_7B_6$ alloy, with the average α-Fe grain size following an 893K heat treatment being only 12 nm.

For the $Fe_{81}Zr_7B_{12}$ alloy the as-quenched sample showed quite similar BF and CDF images and SAD pattern to those of the alloys with lower [B]s. For the sample heated to 883K, i.e., immediately after the first peak on the DSC curve, the BF image (Fig. 4 (upper micrograph)) showed a fairly uniform distribution of crystalline grains. The average grain size was 35 nm. The SAD pattern of the crystalline grains of this alloy (Fig. 4) was clearly more complex than those of the alloys with lower [B]s, which is consistent with the results of the XRD analyses.

When the temperature was increased to 936K (Fig. 4 (lower)), the distribution of the crystalline grains remained unchanged, but the grain size was increased to an average of 42 nm. On increasing the temperature further to 953K, the average grain size was roughly the same, although the SAD pattern showed that the strongest ring became sharper, i.e., the halo effect became weaker, suggesting that the volume fraction of the amorphous matrix was

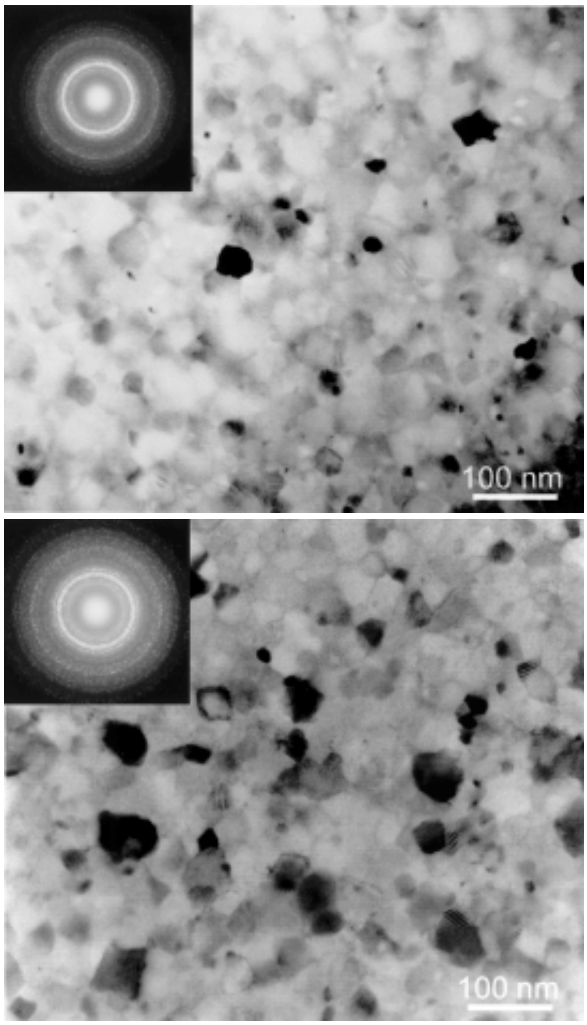

Fig. 4. TEM bright field images and SAD patterns for the nanocrystalline $Fe_{81}Zr_7B_{12}$ alloy heated to 883K (upper) and 936K (lower) at 20 K/min.

reduced. Extensive studies of the changes to the microstructure following isothermal heat treatments have been undertaken and the results of these reported elsewhere [10].

To substantiate the identity and the crystal structure of the metastable crystalline phase, electron microdiffraction and associated computer simulation have been employed. The results from these are also presented elsewhere [10]. It suffices to report that the metastable phase with the cubic "$Fe_{12}Si_2ZrB$" ($I\bar{4}3m$) structure has been confirmed.

4. CONCLUSIONS

For $Fe_{93-x}Zr_7B_x$ alloys with [B] in the range 3 to 6 at.%, the crystalline phase present after the primary crystallization during continuous heating, was the bcc α-Fe phase. The average grain size was 14 nm

for the $Fe_{90}Zr_7B_3$ alloy heated to 875K at 20 K/min and 12 nm for the $Fe_{87}Zr_7B_6$ alloy heated to 893K at 20 K/min. However, for higher [B] (12 at.%) the primary crystalline phase formed on continuous heating was a metastable phase with the cubic "$Fe_{12}Si_2ZrB$" structure. The average grain size of this phase was 35 nm for the alloy heated to 883K at 20 K/min. When the temperature was increased to 1003K, the metastable phase and the residual amorphous phase started to transform into the equilibrium bcc α-Fe and fcc $ZrFe_2$ phases.

ACKNOWLEDGMENTS

X.Y. Xiong acknowledges the financial support of a Monash Graduate Scholarship and an Overseas Postgraduate Research Scholarship. The authors also thank Dr. J.F. Nie for experimental assistance and Dr. K. Suzuki, of the University of New South Wales, for valuable discussions.

REFERENCES

[1] K. Suzuki, A. Makino, A. Tsai, A. Inoue and T. Masumoto // *Mater. Sci. and Eng.* **A179/ A180** (1994) 501.
[2] K.Y. Kim, T.H. Noh, I.K. Kang and T. Kang // *Mater. Sci. and Eng.*, **A179/A180** (1994) 552.
[3] K. Suzuki, A. Makino, N. Kataoka, A. Inoue and T. Masumoto // *Mater. Trans. JIM* **32** (1991) 93.
[4] K. Suzuki, A. Makino, A. Inoue and T. Masumoto // *J. Appl. Phys.* **70** (1991) 6232.
[5] B.D. Cullity, *Elements of X-ray Diffraction* (Addison-Wesley, USA, 1959).
[6] Y. Zhang, K. Hono, A. Inoue, A. Makino and T.Sakurai // *Acta Mater.* **44** (1996) 1497.
[7] M.Kopcewicz, A.Grabias, P.Nowicki and D.L.Williamson // *J. Appl. Phys.* **79** (1996) 993.
[8] T.B. Massalski, *Binary Alloy Phase Diagrams*, 2nd ed., (ASM International, 1990).
[9] H. Okamoto, *Phase Diagrams of Binary Iron Alloys* (ASM International, 1993).
[10] X.Y. Xiong, T.R. Finlayson and B.C. Muddle // *Phil. Mag. A* (2001) (in press).